

# Study of the Mechanism and Rate of Bismaleimide Cure by Remote in-Situ Real Time Fiber Optic Near-Infrared Spectroscopy

Jovan Mijović\* and Saša Andjelić

Department of Chemical Engineering, Polytechnic University, Six Metrotech Center, Brooklyn, New York 11201

Received April 21, 1995; Revised Manuscript Received October 19, 1995<sup>®</sup>

**ABSTRACT:** An investigation was carried out on the mechanism and kinetics of cure of a two-component bismaleimide formulation, composed of 4,4'-methylenbis[maleimidobenzene] and 2,2'-diallylbisphenol A. In-situ real time study of the progress of reaction was conducted in the temperature range from 140 to 250 °C using remote fiber optic near-infrared spectroscopy. The obtained signal was clean, free of noise, and remarkably reproducible. The principal reaction observed was an alternating copolymerization involving maleimide and allyl double bonds. Maleimide homopolymerization was detected only in the initial stages of reaction at temperatures above 200 °C. The extent of self-condensation (or etherification) of hydroxyl groups on the allyl component, which leads to cross-linking, was observed to vary with reaction temperature, suggesting a path to tailor-making networks with desired morphology and physical/mechanical properties.

## Introduction

Bismaleimide (BMI) resins have evolved as an important matrix for polymer composites because of their "epoxy-like" processing characteristics and superior thermal stability and fatigue resistance at high humidity.<sup>1–3</sup> In recent years many "modified" BMI resins have been developed to increase the toughness of these inherently brittle materials.<sup>4,5</sup> Most common BMIs, including those supplied by Rhone-Poulenc, Ciba-Geigy, Shell Chemical Co., and others, contain 4,4'-methylenbis[maleimidobenzene] as one major component and an aromatic diamine, a diallyl alcohol, or another bismaleimide as the other, though a variety of polyfunctional, oligomeric, and toughened BMIs have also been reported.<sup>5–10</sup>

Despite the current popularity of BMIs, there is a paucity of fundamental information about the mechanisms and rates of their cure, which is actually not surprising when one considers the multitude and complexity of the existing BMI formulations. Published reports of direct relevance to our BMI formulation are cited throughout the text. Several kinetic investigations based on the use of differential scanning calorimetry (DSC) have been reported,<sup>10–13</sup> though they provide only phenomenological information and shed little light on the reaction mechanism. A review of the literature on reactions in various maleimide and bismaleimide systems, polymer-forming and non-polymer-forming alike, has revealed a number of proposed reaction paths in BMI formulations, though a comprehensive picture of the mechanisms and kinetics of cure has not yet emerged. The following reactions have been suggested to occur during cure of various BMI formulations: (1) homopolymerization of BMI via the reaction of maleimide C=C double bond that results in the formation of a four-member ring structure,<sup>14</sup> (2) homopolymerization of BMI via the reaction of maleimide C=C double bond between three BMI molecules,<sup>15</sup> (3) reactions between the double bonds of maleimide and allyl groups, which continue at higher temperature via Diels–Alder

mechanism and maleimide oligomerization,<sup>16</sup> (4) reaction of bismaleimide with allyl component and/or another bismaleimide molecule via a free radical site on the methylene group,<sup>17</sup> (5) homopolymerization (vinyl-type) of the allyl double bond, and (6) cross-linking via etherification (dehydration) involving hydroxyl groups of the allyl component.<sup>13</sup>

The principal objective of this study is to investigate the mechanism and kinetics of cure of a two-component BMI formulation, composed of 4,4'-methylenbis[maleimidobenzene] and 2,2'-diallylbisphenol A, using in-situ real time fiber optic near-infrared (IR) spectroscopy. An understanding of the reaction mechanism and kinetics is a prerequisite for the development of process models, which, in turn, are of crucial importance to the process engineers engaged in optimization of processes and products. This is the first report in the literature on the use of near-IR spectroscopy to study the cure of a BMI formulation, although mid-IR spectroscopy has been used to investigate polymer morphology (e.g., orientation and crystallization, ref 18).

## Experimental Section

**Materials.** A two-component BMI system (Matrimid 5295; courtesy of Ciba-Geigy Corp.), consisting of 4,4'-methylenbis[maleimidobenzene] (component A) and 2,2'-diallylbisphenol A (component B), was utilized in this study. Equimolar amounts of components were mixed at 120–125 °C and stirred continuously until a clear, homogeneous solution was obtained. Reaction kinetics were studied at a series of temperatures between 140 and 250 °C. Several model compounds were used for the identification of IR absorption peaks, including a maleimide monomer (99%+; Aldrich), allyl acetate, styrene, phenol, diglycidyl ether of bisphenol A, and 4,4'-methylenedianiline. Chemical structures of the BMI formulation components and maleimide monomer are shown in Figure 1.

**Technique—Remote Fiber Optic Near-IR Spectroscopy.** A Nicolet Magna-IR System 750 Fourier transform infrared spectrometer, with spectral range coverage from 15 800 to 50 cm<sup>-1</sup> and a Vectra scanning interferometer with better than 0.1 cm<sup>-1</sup> resolution, was used in this study. Near-IR data were obtained using a calcium fluoride beamsplitter, a white light source, and an MCT detector cooled with liquid nitrogen. All spectra were measured at 4 cm<sup>-1</sup> resolution using 35 scans. A schematic presentation of our experimental setup is given in Figure 2A.

\* To whom correspondence should be addressed.

<sup>®</sup> Abstract published in *Advance ACS Abstracts*, December 1, 1995.

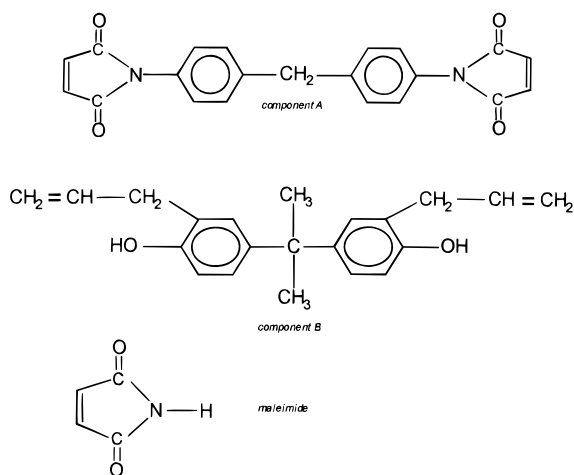


**Figure 1.** Chemical structure of 4,4'-methylenebis[maleimido]benzene (component A), 2,2'-diallylbisphenol A (component B), and maleimide monomer.

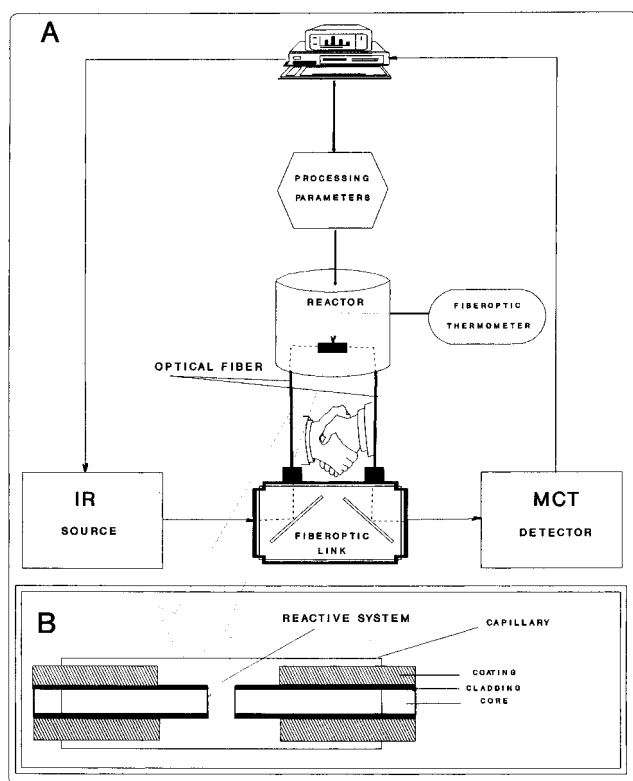


**Figure 2.** (A) Schematic of remote fiber optic near-IR spectroscopy assembly. (B) Schematic of optical fiber/capillary disposable cell configuration.

A large core (600/630  $\mu\text{m}$ ) low-OH-fused silica-type multi-mode optical fiber (3 M specialty optical fiber) was used. The fiber was characterized by an attenuation at 630 nm of  $<50$  dB/km and a numerical aperture of  $0.39 \pm 0.02$ . Two lengths of the fiber (lengths of up to 10 m were successfully tested) were utilized as receiving and transmitting legs. An optical fiber link containing reflective mirrors was used to couple the signal into the transmitting leg and out of the receiving leg. SMA connectors (Newark Electronics) were utilized to attach fiber legs to the fiber link. At the sample side, two distal fiber ends were axially centered and positioned to face each other. Depending on the type and size of sample, several disposable cell configurations were designed and successfully tested. All had an adjustable path length, enabling us to optimize the signal. In most instances, a path length of 2–3 mm was sufficient for excellent transmission and a clear near-IR absorption signal down to  $4000\text{ cm}^{-1}$ . The results shown in this column were generated using the optical fiber/capillary

configuration, schematically shown in Figure 2B. A short length ( $<10$  mm) of protective buffer was removed from the distal ends of transmitting and receiving fiber legs, which were then slipped into the capillary to a desired path length. The space between fiber ends was filled with the reactive mixture free of bubbles, and the whole assembly was inserted into a programmable temperature-controlled chamber. A highly accurate measurement of the sample temperature is essential in kinetic studies, and that places a premium on the experimental precision. Temperature during reaction was monitored with a Luxtron 750 multichannel fluoroptic thermometer, by placing the tip of its optical fiber probe in direct contact with the portion of capillary filled with the reactive mixture.

The above-described experimental procedure is very attractive; it features a simple design, low cost, small sample size, short preparation time, in-situ real time response, and remarkable reproducibility and reliability of data. Most importantly, however, the cell is disposable, in contrast to several recently marketed and quite expensive commercial fiber optic probes (e.g., Nicolet/Spectra Tech, Axion, Guided Wave) that are nondisposable and hence cannot be used to monitor processing of thermoset polymers and composites. In fact, the information provided in this communication is probably sufficient to enable interested researchers to assemble their own remote fiber optic near-IR setups at a fraction of the cost of commercial probes. After curing of our sample, a small length of the optical fiber embedded in the cured resin was cleaved and the new ends were polished to a clean mirror-flat surface for the next run. Further details of our experimental procedure are available elsewhere.<sup>19</sup>

## Results and Discussion

The presentation and discussion of results is divided into four sections. In the first section we establish the location and origin of the characteristic near-IR absorption bands. The mechanism and the reaction kinetics are discussed in section 2 for the temperature range from 140 to  $200\text{ }^{\circ}\text{C}$  and in section 3 for the temperature range from 200 to  $250\text{ }^{\circ}\text{C}$ . Etherification involving two hydroxyl groups, which leads to cross-linking, is discussed in section 4.

**1. Identification and Assignment of the Characteristic Near-IR Absorptions.** We begin our discussion by presenting room temperature near-IR spectra of 4,4'-methylenebis[maleimido]benzene (component A) and 2,2'-diallylbisphenol A (component B), in Figures 3 and 4, respectively. We stress that the identification and assignment of the characteristic absorptions in this system were further supported by the evidence from near-IR spectra of a series of model compounds, including maleimide, allyl acetate, phenol, diglycidyl ether of bisphenol A, and 4,4'-methylenedianiline, as well as the mid-IR spectra of our components A and B and their mixtures.

Two characteristic peaks at  $6089$  and  $4871\text{ cm}^{-1}$ , observed in component A (Figure 3) and assigned to the maleimide double bond, are the overtones of fundamental mid-IR absorptions at  $3100$  and  $1900\text{ cm}^{-1}$ , respectively. The unusually high frequency range of the latter peak in comparison with the location of double-bond absorption in aromatic (e.g., benzene) or aliphatic compounds, where it is located typically between  $1800$  and  $1600\text{ cm}^{-1}$ , is attributed to the presence of two strong acceptors, i.e., carbonyl groups, in the maleimide ring.

Room temperature near-IR spectra of component B (Figure 4) show three distinct characteristics: (1) the absorption band at  $6917\text{ cm}^{-1}$ , which represents free and hydrogen-bonded OH stretching vibration of the bisphenol A moiety, (2) the peak at  $6114\text{ cm}^{-1}$ , identified as an overtone of the aliphatic double bond of the allyl

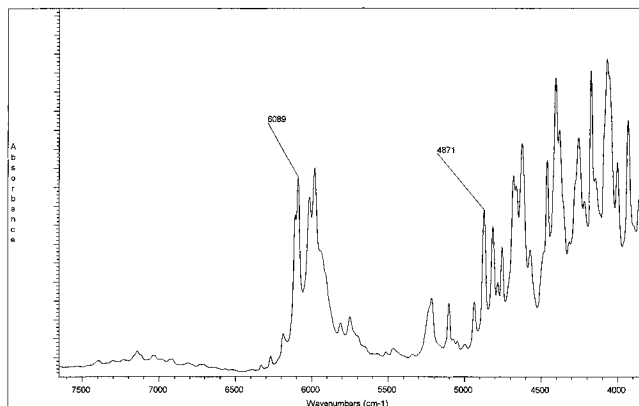


**Figure 3.** Near-IR spectrum of 4,4'-methylenebis[maleimido-benzene] (component A) at room temperature.

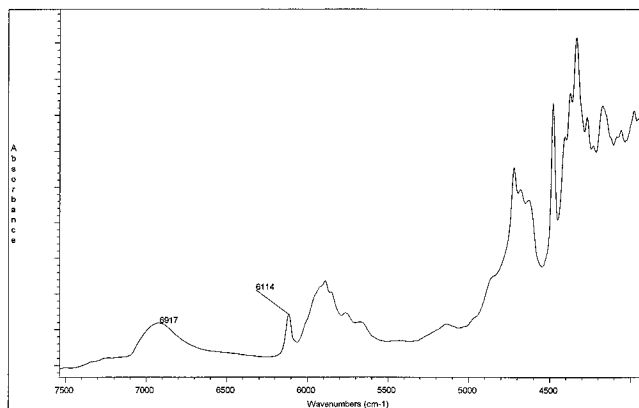


**Figure 4.** Near-IR spectrum of 2,2'-diallylbisphenol A (component B) at room temperature.

group only (double bond of the benzene ring absorbs around  $6000\text{ cm}^{-1}$  and does not overlap with the band at  $6114\text{ cm}^{-1}$ ), and (3) a weak overtone of the OH deformation band which absorbs at the same frequency as the maleimide double bond at  $4871\text{ cm}^{-1}$  and thus becomes particularly important in the kinetic analysis based on the disappearance of maleimide double bonds. We shall elaborate on this point later in the text.

Prior to mixing components A and B, each was examined separately for a possible homopolymerization at high temperature. Instead of component A, however, whose high melting point of  $160\text{ }^{\circ}\text{C}$  caused experimental difficulties in our capillary sample configuration, we utilized the maleimide monomer (Figure 1) as a model compound. We observed no changes in the near-IR spectra of this compound at temperatures as high as  $200\text{ }^{\circ}\text{C}$  and for times as long as 30 min and concluded that homopolymerization did not take place under these conditions.

Interesting results were obtained in the investigation of a homopolymerization of component B. As stated above, we have noted two characteristic hydroxyl absorption bands in the room temperature near-IR spectrum of component B (Figure 4), a strong one at  $6917\text{ cm}^{-1}$  and a weak one at  $4871\text{ cm}^{-1}$ . Upon heating, the former shifts to a higher frequency while, at the same time, its absorption intensity increases. Curiously, the latter peak does not shift along the frequency axis, but its intensity also increases with temperature. Most importantly, however, the observed effect is reversible and strictly thermally activated up to  $250\text{ }^{\circ}\text{C}$ , i.e., for a fixed isothermal condition no change is observed with time. The onset of homopolymerization via allyl double

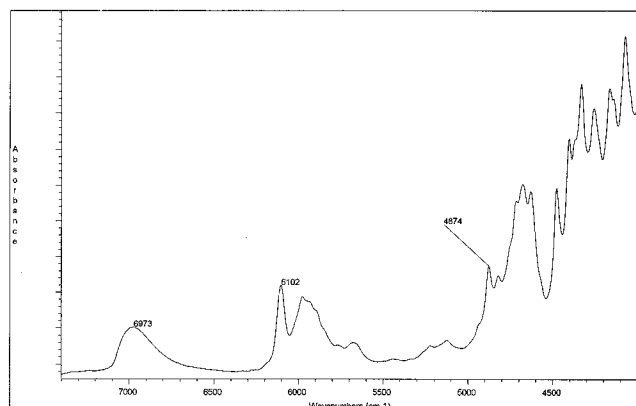


**Figure 5.** Near-IR spectrum of BMI formulation at  $140\text{ }^{\circ}\text{C}$ .

bonds was observed at ca.  $250\text{ }^{\circ}\text{C}$ , in complete agreement with the results of DSC, reported by our group<sup>11</sup> and other investigators.<sup>13,20</sup>

A spectrum of the mixture of components A and B (i.e., our BMI formulation) at  $140\text{ }^{\circ}\text{C}$  prior to the onset of reactions is shown in Figure 5. A shift in the absorption due to OH stretching vibrations from  $6917\text{ cm}^{-1}$  (where it appears in component B at room temperature) to  $6973\text{ cm}^{-1}$  (upon mixing of the formulation at  $140\text{ }^{\circ}\text{C}$ ) is attributed solely to the temperature effect. This is readily confirmed by the additional shifts of this peak to higher frequency at still higher temperature (e.g., at  $200\text{ }^{\circ}\text{C}$  the peak shifts to  $7002\text{ cm}^{-1}$ ). On the basis of these results and the corroborative evidence from our earlier analyses of a series of reactive systems (e.g., bisphenol A-type epoxies) and model compounds (e.g., maleimide, phenol, allyl acetate, styrene), we believe that the underlying mechanism for the observed shifts is the transition of hydrogen-bonded to free OH absorption upon heating. Naturally, this process was reversible upon cooling. It is also interesting to point out that this phenomenon cannot be easily seen in the mid-IR spectra, where the ratio of "free" to "bonded" hydroxyl absorption is about 30 times lower than in the near-IR range.<sup>21</sup>

The observed temperature dependence of hydroxyl absorption is more pronounced in bismaleimide resins than in epoxies, suggesting a presence of multiple intra- and intermolecular hydrogen-bonded complexes involving the OH group, of which the following are likely to dominate (1) OH...OH interactions, which appear in the near-IR spectra of phenol (a model compound), for example, as a broad shoulder on the free OH absorption peak at  $6933\text{ cm}^{-1}$ , (2) OH...allyl double-bond interactions, which are enhanced by the short distance between them in component B, and (3) OH...carbonyl interactions, which are a well-known form of intermolecular hydrogen bonding often associated with improved miscibility in mixtures and blends.

The non-benzene CH=CH double-bond absorption, observed at  $6089$  (Figure 3) and  $6114$  (Figure 4)  $\text{cm}^{-1}$  in the room temperature near-IR spectra of components A and B, respectively, appears at  $6102\text{ cm}^{-1}$  in the near-IR spectrum of the initial bismaleimide formulation shown in Figure 5. Since this absorption comprises both maleimide and allyl double bonds in components A and B, it can be utilized in kinetic studies as a measure of the overall concentration of non-benzene double bonds in the formulation at any time. In contrast, the peak at  $4874\text{ cm}^{-1}$  in the BMI formulation (Figure 5) and its counterpart at  $4871\text{ cm}^{-1}$  in component A (Figure 3)

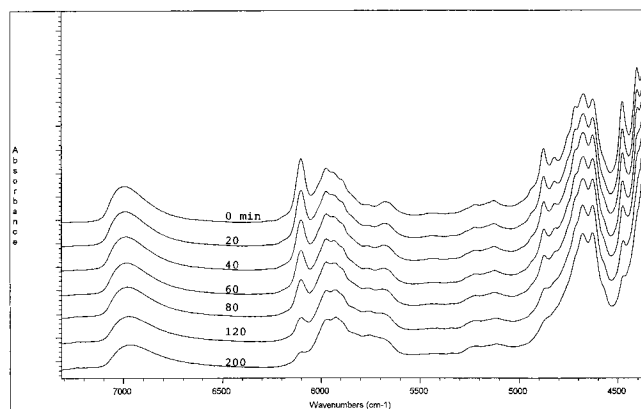


**Figure 6.** Near-IR spectra of BMI formulation at various times during cure at 180 °C.

represent only the maleimide double bond and a small overlapping contribution due to hydroxyl absorption which is described later in the text. This important distinction enabled us to distinguish between the rate of disappearance of maleimide double bonds and allyl double bonds at various temperatures and to shed light on the mechanism of reaction between components A and B.

**2. Reaction Kinetics in the Temperature Range between 140 and 200 °C.** We begin this section by emphasizing that all near-IR spectra generated during cure varied in a systematic manner and were invariably sharp, noise-free, and extremely reproducible. An example of the progressive changes in near-IR spectra during isothermal cure at 180 °C is shown in Figure 6. The spectra taken at various stages of cure were shifted along the ordinate for clarity. The following trends, displayed by major peaks of relevance to bismaleimide cure, were evident. (1) A decrease in the OH absorption at 6996  $\text{cm}^{-1}$  (its initial location at 180 °C) was caused by etherification involving two OH groups. The formation of ether linkage has also been confirmed in this study by mid-IR spectroscopy. (2) A decrease in the peak at 6100  $\text{cm}^{-1}$  resulted from the disappearance of both allyl and maleimide double bonds. (3) A decrease in the maleimide double bond absorption occurred at 4874  $\text{cm}^{-1}$ . We should add that an adjacent peak at 4820  $\text{cm}^{-1}$  with the same molecular origin was also observed, but it was weak and hence of a limited use in the kinetic studies. (4) A change in the frequency range between 6000 and 5600  $\text{cm}^{-1}$  due to the varying nature of the C–H absorptions resulted from the gradual conversion of C=C to C–C bonds. A careful examination of near-IR spectra for all stages of cure between 140 and 200 °C showed no qualitative difference between them, suggesting that the same reaction mechanism characterizes cure in that temperature range.

Quantitative evaluation of the reaction kinetics was conducted by following the disappearance of hydroxyl peak (ca. 7000  $\text{cm}^{-1}$ ) and the two double-bond peaks (6100 and 4874  $\text{cm}^{-1}$ ). The benzene ring absorption at 4625  $\text{cm}^{-1}$  was used as a reference. The extent of reaction ( $\alpha$ ) at any time,  $t$ , was calculated from the initial areas of reactive ( $r$ ) and reference ( $\text{ref}$ ) peaks,  $A_{r,0}$  and  $A_{\text{ref},0}$ , respectively, and their corresponding values at time  $t$ ,  $A_{r,t}$  and  $A_{\text{ref},t}$ , respectively, according to the following equation:

$$\alpha = 1 - [(A_{r,t}A_{\text{ref},0}) / (A_{r,0}A_{\text{ref},t})] \quad (1)$$

The normalized extent of reaction based upon the

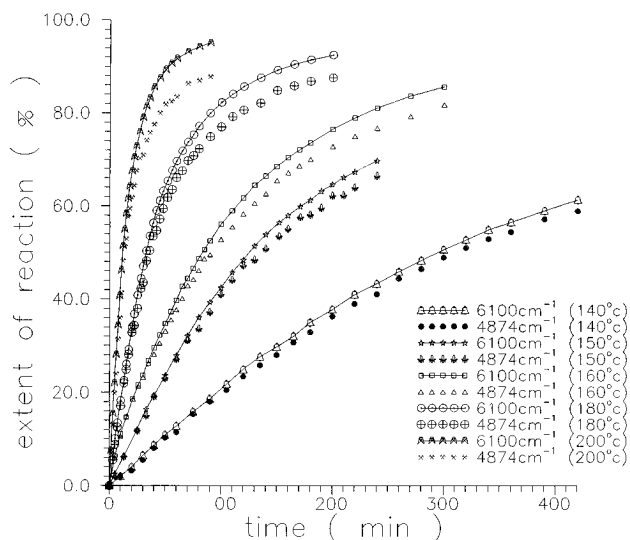


**Figure 7.** Extent of reaction of BMI formulation based upon the consumption of double bonds as a function of time for a series of isothermal runs between 140 and 200 °C.

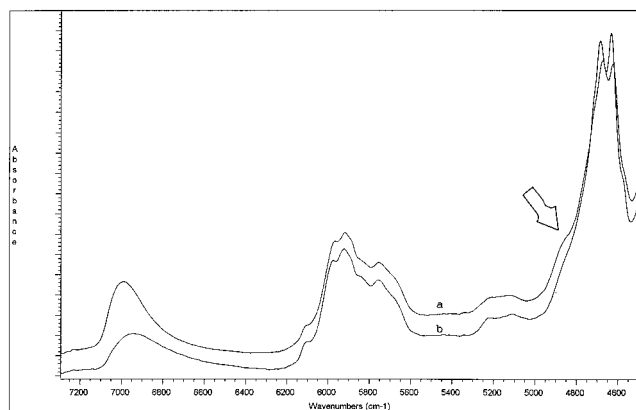


**Figure 8.** Near-IR spectra of BMI formulation in the late stage of cure at 200 °C. Traces a and b represent hot (200 °C) and cold (25 °C) samples, respectively.

consumption of double bonds is shown in Figure 7 as a function of time for isothermal runs at 140, 150, 160, 180, and 200 °C. Solid and dashed lines represent the kinetic results calculated from the normalized rate of disappearance of peaks at 6100 and 4874  $\text{cm}^{-1}$ , respectively. Initially, the two rates were identical. As the reaction progressed, however, we observed a gradual decrease in the reaction rate based on the maleimide group at 4874  $\text{cm}^{-1}$  in comparison to that based on the absorption of all non-benzene-type double bonds at 6100  $\text{cm}^{-1}$ . Considering that the reaction between maleimide and allyl double bonds leads preferentially to the formation of an alternating copolymer (as described below), the observed difference in the normalized extent of reaction based on the peaks at 6100 and 4874  $\text{cm}^{-1}$  was unexpected. After a careful examination of the spectra, we were able to trace the cause of this deviation to the presence of a (very weak) hydroxyl absorption which overlaps with the maleimide peak. The observed discrepancy was more pronounced at higher temperature as a result of an increase in the absorption of free hydroxyl groups with temperature. This phenomenon is exemplified in Figure 8 which shows a near-IR spectrum of our BMI formulation in the late stage of cure at 200 °C, where 99% of maleimide and allyl double bonds have been consumed. Traces a and b represent the spectra of hot (200 °C) and cold (25 °C) samples,

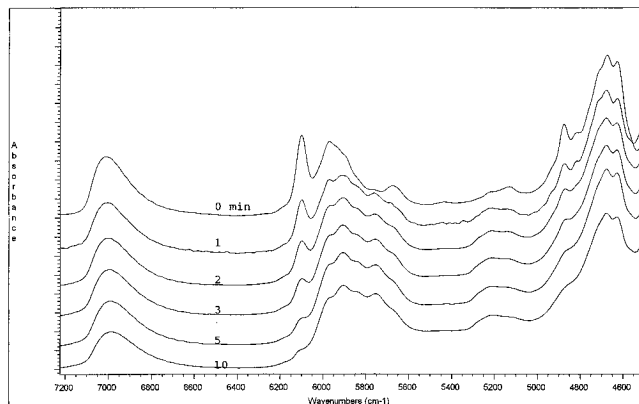


**Figure 9.** Near-IR spectra of BMI formulation at various times during cure at 240 °C.

respectively. The differences in the characteristic hydroxyl absorption regions at 7000 and 4874  $\text{cm}^{-1}$  (see arrow in Figure 8) were clearly evident, and the observed temperature effect was reversible. By using Fourier deconvolution integral, one can further show how the high-frequency shoulder of the 4874  $\text{cm}^{-1}$  peak increases with increasing temperature, as was done for a series of samples. All this evidence points to the presence of a temperature-dependent hydroxyl absorption around 4874  $\text{cm}^{-1}$ , which must be accounted for in the calculations of the rate of disappearance of maleimide double bonds. When this is done, the rates of disappearance of maleimide and allyl double bonds result identical, providing further support to the proposed alternating copolymerization scheme.

**3. Reaction Kinetics in the Temperature Range between 200 and 250 °C.** An example of a systematic change in the near-IR spectra during cure at 240 °C is shown in Figure 9. Identical trends in characteristic absorptions were observed in the spectra collected at other temperatures in this range. The major differences vis-à-vis the spectra obtained at temperatures below 200 °C were noted in the regions of aliphatic C–H stretching absorptions (between 5600 and 6000  $\text{cm}^{-1}$ ) and C–H deformation vibrations (between 4000 and 4600  $\text{cm}^{-1}$ ). For convenience sake, we shall analyze the spectral region near 6000  $\text{cm}^{-1}$ . In an earlier DSC study by Morgan et al.<sup>13</sup> it was correctly suggested that the homopolymerization of 4,4'-methylenebis[maleimido-benzene] (component A) occurs above 200 °C. To confirm these findings by near-IR spectroscopy, we investigated the homopolymerization of maleimide (a model compound) at 240 °C. Near-IR spectra of the initial maleimide monomer and a fully homopolymerized sample are represented by traces a and b, respectively, in Figure 10. The maleimide double-bond peaks at 6100 and 4874  $\text{cm}^{-1}$  disappear completely during reaction, while new peaks at 5900, 5837, and 5756  $\text{cm}^{-1}$  appear in the spectra of a fully polymerized maleimide. Further relevant information was obtained by comparing the spectra of the bismaleimide formulation immediately upon mixing at 180 °C (trace a), after complete cure at 180 °C (trace b), and after complete cure at 240 °C (trace c), all of which are displayed in Figure 11. The three new peaks in the sample cured at 240 °C, which appear at 5901, 5840, and 5752  $\text{cm}^{-1}$ , correspond precisely to those observed in the homopolymerized maleimide model compound and thus provide a clear proof of the homopolymerization of component A above 200 °C.

Additional evidence for the homopolymerization of maleimide double bond can be deduced from Figure 12,

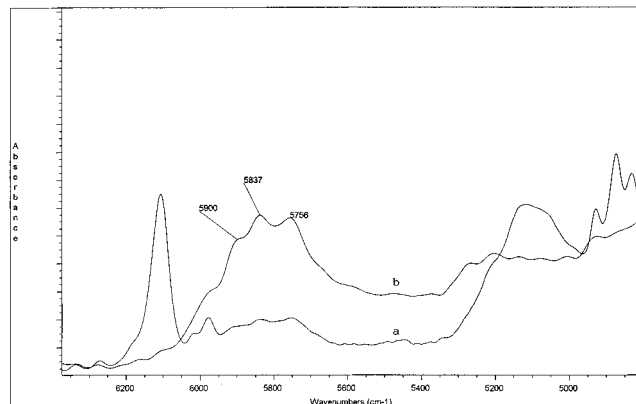


**Figure 10.** Near-IR spectra of the initial maleimide monomer (trace a) and a fully homopolymerized sample (trace b).

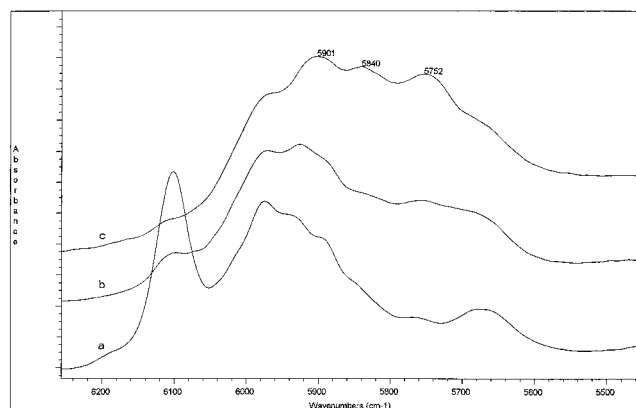


**Figure 11.** Near-IR spectra of BMI formulation immediately upon mixing at 180 °C (trace a), after complete cure at 180 °C (trace b), and after complete cure at 240 °C (trace c).

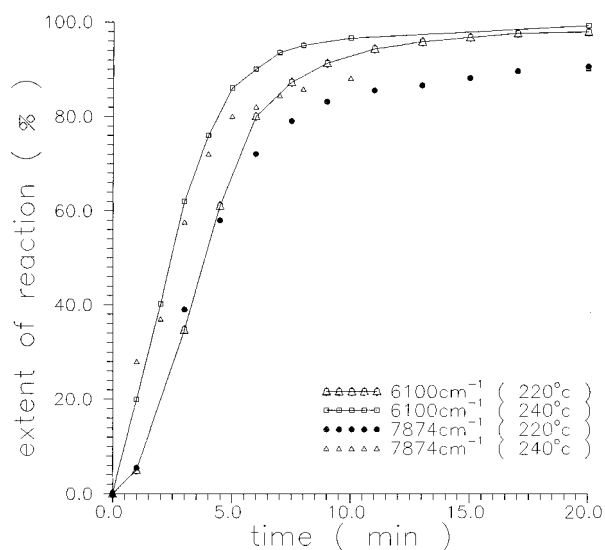


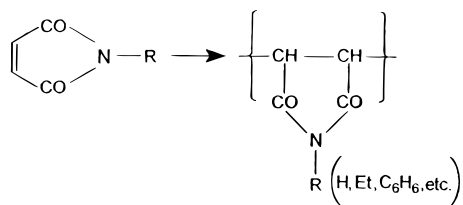
**Figure 12.** Extent of reaction of BMI formulation based upon the consumption of double bonds as a function of time for isothermal runs at 220 and 240 °C.

which shows the extent of reaction of our BMI formulation at 220 and 240 °C calculated from the rates of disappearance of double-bond absorptions at 6100 and 4874  $\text{cm}^{-1}$ . We reiterate here that the former peak encompasses both maleimide and allyl double-bond absorptions, whereas the latter peak represents only the maleimide double bond. A careful examination of data at both temperatures (Figure 12) reveals an initial period where the rate of maleimide consumption is faster than the rate of reaction of maleimide and allyl

double bonds combined. The initial extent of reaction based on the maleimide peak at  $4874\text{ cm}^{-1}$  is ca. 8% higher after 1 min at  $240^\circ\text{C}$  and ca. 5% higher after 3 min at  $220^\circ\text{C}$  in comparison with the results based upon the  $6100\text{ cm}^{-1}$  peak. The reproducibility of these experimental findings was repeatedly verified and is not in doubt. Following this initial period, at the extent of reaction of about 30% at  $240^\circ\text{C}$  and 45% at  $220^\circ\text{C}$ , the rate of consumption of double bonds reverts to the dominant trend observed at all stages of cure, i.e., the alternating copolymerization of maleimide and allyl double bonds.

To lend further support to the suggested fast *initial* homopolymerization of the maleimide double bond *above*  $220^\circ\text{C}$ , we have performed the following experiment. A sample was cured at  $180^\circ\text{C}$  to ca. 30% conversion based upon the  $6100\text{ cm}^{-1}$  peak. The reaction temperature was then suddenly increased to  $250^\circ\text{C}$ . The reaction mixture reached that temperature in less than 1 min, and we continued to record the spectra until the double-bond peaks completely vanished. A comparison of the spectrum generated at the end of cure at  $250^\circ\text{C}$  with the corresponding spectra at  $180^\circ\text{C}$  revealed identical results, suggesting that the fast initial homopolymerization of maleimide cannot be induced by raising the temperature once the reactions have advanced beyond some critical extent. This finding was interpreted as additional proof that the maleimide homopolymerization was limited to the initial stage (high monomer concentration) of reaction and to temperatures above  $200^\circ\text{C}$ .

There is ample experimental evidence in the literature<sup>22</sup> to show that a maleimide can homopolymerize more readily than, for instance, maleic anhydride and that nonsubstituted maleimides (i.e.,  $R = \text{H}$ , see below) do not undergo a polyaddition reaction involving the double bond and the N–H bond. The homopolymerization of 4,4'-methylenebis[maleimidobenzene] (component A) proceeds according to the following scheme:

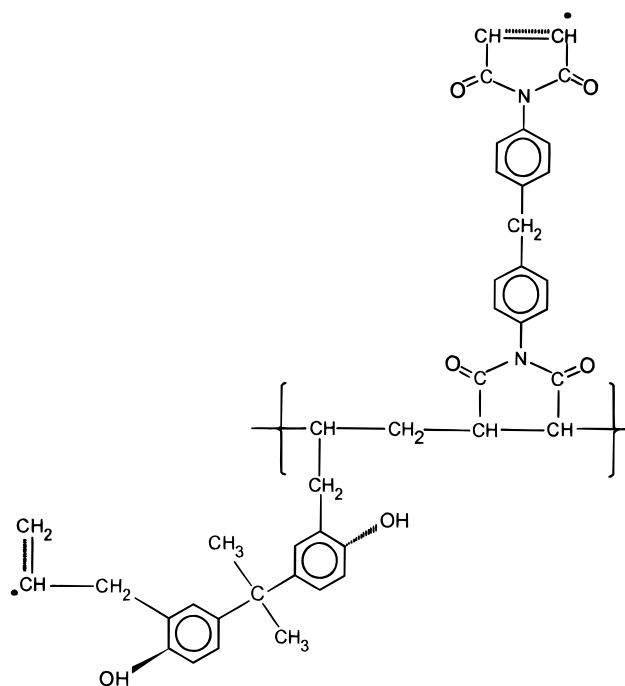


Our principal findings up to this point can be summarized as follows. Experimental evidence based upon the rate of disappearance of double bonds suggests that the principal reaction is this BMI formulation in the temperature range between  $140$  and  $250^\circ\text{C}$  involves copolymerization between maleimide and allyl double bonds. This is, in fact, the only reaction that involves double bonds below  $200^\circ\text{C}$ . It also dominates the temperature range above  $200^\circ\text{C}$ , except for an initial stage characterized by a fast homopolymerization of maleimide. The supporting evidence for this reaction path abounds. First, when the presence of a weak hydroxyl absorption near the maleimide peak at  $4874\text{ cm}^{-1}$  is correctly accounted for, we find that the normalized rates of consumption of non-benzene double bonds in components A and B below  $200^\circ\text{C}$  are equal. Second, we have established that maleimide and allyl double bonds (absorption at  $6100\text{ cm}^{-1}$ ) are almost completely consumed, even at temperatures below  $200^\circ\text{C}$ ; for instance, 93% and 98% conversion are found at the end

of reaction at  $180$  and  $200^\circ\text{C}$ , respectively. Third, the observed homopolymerization of maleimide is limited to the initial stage of reaction at temperatures above  $200^\circ\text{C}$ , and fourth, the use of excess (25%) of either component revealed the presence of *that component only* at the end of cure.

The propensity for copolymerization in compounds similar to our components A and B is well documented in the literature.<sup>23</sup> Due to strong electron acceptor properties of the carbonyl group, compounds like maleic anhydride (and maleimides) can copolymerize with a variety of donor molecules, such as hydrocarbons, to form alternating copolymers. Although our literature search did not yield a value of the reactivity ratio for the pair of components (A and B) of the BMI formulation utilized in this work, we were able to deduce a supporting evidence from the reported values for chemically similar pairs. For instance, maleimide monomer has been shown to react with styrene,  $\alpha$ -methylstyrene, and allyl acetate to produce an almost perfect alternating copolymer. The reactivity ratio product ( $r_1 r_2$ ) for maleimide–allyl acetate pair was reported to be 0.000 54, very close to zero—the value for a perfectly alternating copolymer.

On the basis of the above presented findings that combine the evidence from near-IR, mid-IR, DSC, and TGA, we believe that the following structure represents the principal product of reactions involving double bonds in our formulation:



We further believe that, in the course of copolymerization, 2,2'-diallylbisphenol A (component B) follows the "1,2" rather than the "2,3" type mechanism. This result, which was intuitively expected because of the strong steric hindrance and polarity of the hydroxyl group, has been experimentally confirmed by the absence of substantial increase in the  $\text{CH}_3$  group absorption in the near-IR spectra, which otherwise would have taken place.

**4. Reactions Involving Hydroxyl Groups.** The final portion of our discussion is devoted to the interesting findings that concern the consumption of hydroxyl groups on 2,2'-diallylbisphenol A (component B) in our

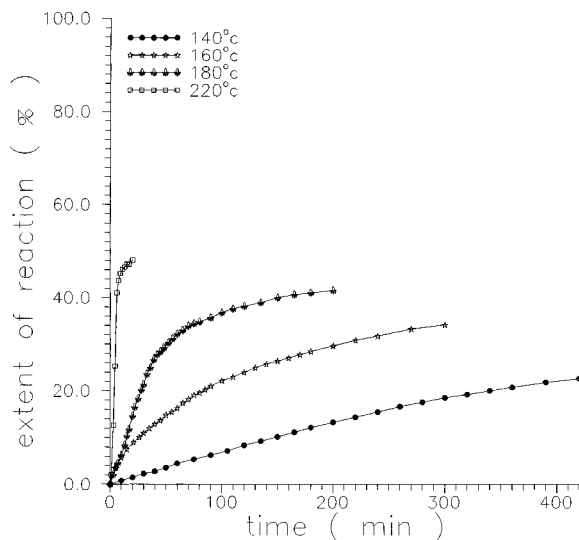


**Figure 13.** Extent of reaction of hydroxyl groups in BMI formulation as a function of time for a series of isothermal runs between 140 and 220 °C.

BMI formulation. By monitoring a decrease in the hydroxyl group absorption near  $7000\text{ cm}^{-1}$ , we were able to establish that the etherification reaction, which leads to cross-linking and is accompanied by water evaluation, does occur at a measurable rate in the BMI formulation (but not in component B alone), even at a temperature as low as 140 °C. These tests were repeated a number of times, and the accuracy and reproducibility of data are not in question. The extent of reaction of hydroxyl group, calculated using an equation analogous in form to eq 1, is shown in Figure 13 for a series of temperatures between 140 and 220 °C. It is obvious from Figure 13 that the etherification reaction cannot be neglected; the consumption of hydroxyl groups reaches 20% after 6 h at 140 °C and 45% after 10 min at 200 °C! Further corroborating evidence for this reaction was obtained from the observed increase in ether absorption in the mid-IR spectra and the visual observation of bubble formation during reaction. The amount of bubbles was found to increase with time. The observed dehydration also agrees well with the results of thermogravimetric analysis (TGA) of the same bismaleimide formulation reported by Morgan et al.<sup>13</sup> The initial weight loss at 130 °C coincides with the onset of dehydration which proceeds at an increasing rate before leveling off at about 260 °C as a result of diffusion limitations in the vitrified network. The abrupt weight loss above 350 °C can be explained by addition dehydration and a simultaneous initiation of degradation, albeit the elucidation of the corresponding mechanism warrants further research.

The observation that OH groups react with each other well below 200 °C in the BMI formulation (components A and B combined), but do not react with each other in component B alone up to ca. 250 °C, is quite intriguing. Explanations for such behavior in chemically similar compounds have been offered in the literature in terms of electron donor/acceptor transfer mechanisms and transition complexes.<sup>12</sup> Further in-depth, consideration of this phenomenon, however, was beyond the scope of this study.

The rate of etherification was also investigated for two BMI formulations with a 25% molar excess of either component. With component A in excess, no difference was observed in comparison with the stoichiometric

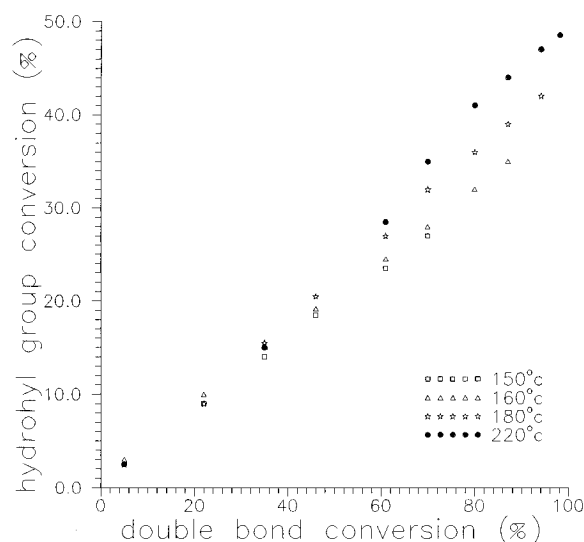


**Figure 14.** Cross-plot of extent of reaction of BMI formulation based upon the conversion of hydroxyl groups versus double bonds, with reaction temperature as a parameter.

formulation. In the formulation with component B in excess, we observed a decrease in the conversion of hydroxyl group on the order of 25–30%, suggesting that the etherification reaction in the BMI formulation requires the presence of a 1:1 complex formed by a pair of components A and B and that the “unpaired” hydroxyl groups on component B remain inactive below 250 °C.

Finally, interesting information can be inferred about the cross-link density of cured networks by looking into the effect of temperature on etherification. In Figure 14, which is quite revealing, we show a plot of hydroxyl group conversion (extracted from Figure 13) as a function of double-bond conversion (extracted from Figure 12), with temperature as a parameter. Note that the conversion of double bonds in this figure approaches 100%, while that of hydroxyl groups remains below 50%. It is apparent from Figure 14 that for a given double-bond conversion: (1) the extent of hydroxyl conversion increases with increasing temperature and (2) the difference between hydroxyl conversion at low and high ends of the temperature range increases with increasing double-bond conversion. For example, a 20% double-bond conversion, hydroxyl conversion increases by about 2% in going from 150 to 220 °C, while at an 80% double-bond conversion the corresponding increase exceeds 8%. Since the extent of hydroxyl conversion (i.e., etherification) determines the cross-link density, it is suggested that the network morphology and its physical/mechanical properties could be controlled by controlling the thermal history during cure.

## Conclusions

We have completed an investigation of the mechanism and rate of cure of a bismaleimide formulation composed of 4,4'-methylenebis[maleimidobenzene] and 2,2'-diallylbisphenol A. Experiments were conducted in the temperature range from 140 to 250 °C using in-situ real time fiber optic near-IR spectroscopy. Several characteristic near-IR absorption peaks were identified and utilized to evaluate the reaction kinetics: a peak at  $6100\text{ cm}^{-1}$  due to maleimide and allyl double bonds, a peak at  $4874\text{ cm}^{-1}$  due to maleimide double bonds only, and a peak at ca.  $7000\text{ cm}^{-1}$  due to hydroxyl groups. The principal reaction path involves an alternating copolymerization of maleimide and allyl double bonds.

Homopolymerization of maleimide double bonds was noted only during the initial stage of reaction above 200 °C. Self-condensation (i.e., etherification) of hydroxyl groups on the diallyl component, which leads to cross-linking and is accompanied by evolution of water, was found to occur in the entire temperature range studied. The observed interplay between the conversion of double bonds and hydroxyl groups depends on the thermal history during cure and could be utilized to control the morphology and physical/mechanical properties of cured networks.

**Acknowledgment.** Funding provided by the Air Force Office of Scientific Research under Grant No. F49620-93-1-0603 is gratefully acknowledged.

## References and Notes

- (1) Stenzenberger, H. D. In *Structural Adhesives: Developments in Resins and Primers*; Kinloch, A. J., Ed.; Elsevier Applied Science: Amsterdam, 1986.
- (2) Sillion, B. In *Comprehensive Polymer Science*; Allen, G., Bevington, J. C., Eds.; Pergamon Press: Oxford, 1989; Vol. 5.
- (3) Chattha, M. S.; Dickie, R. A. *J. Appl. Polym. Sci.* **1990**, *40*, 411.
- (4) Stenzenberger, H. D.; Romer, W.; Hergenrother, P. M.; Jensen, B.; Breitigam, W. *SAMPE J.* **1990**, *26* (6), 75.
- (5) Recent advances have been discussed at the Symposium on Toughened Plastic, American Chemical Society Meeting, March 1994, San Diego, CA; *Proc. Polym. Mater. Sci. Eng.* Vol. 70.
- (6) Pilato, L. A.; Michno, J. *Advanced Composite Materials*; Springer-Verlag: Heidelberg, 1994.
- (7) Donnellan, T. M.; Roylance, D. *Polym. Eng. Sci.* **1992**, *32* (6), 409.
- (8) Donnellan, T. M.; Roylance, D. *Polym. Eng. Sci.* **1992**, *32* (6), 415.
- (9) Barrett, K. A.; Fu, B.; Wang, A. Proceed. 35th Intl. SAMPE Symp., April 2–5, 1990; p 1007.
- (10) Lin, K.-F.; Lin, J.-S. *J. Appl. Polym. Sci.* **1993**, *50*, 1601.
- (11) Mijovic, J.; Schafran, B. *SAMPE J.* **1990**, *26*, 51.
- (12) Nagai, A.; Takahashi, A.; Suzuki, M.; Katagiri, J.; Mukoh, A. *J. Appl. Polym. Sci.* **1990**, *41*, 2241.
- (13) Morgan, R. J.; Jurek, R. J.; Yen, A.; Donnellan, T. *Polymer* **1993**, *34* (4), 835.
- (14) Lee, B.; Chaudhari, M. A.; Galvin, T. *Int. SAMPE Tech. Conf.* **1985**, *17*, 172.
- (15) Lind, A. C.; Fry, C. G. *ACS Proc. Div. Polym. Mater. Sci. Eng.* **1988**, *59*, 466.
- (16) King, J. J.; Chaudhari, M.; Zahir, S. *Int. SAMPE Symp.* **1984**, *29*, 394.
- (17) Brown, I. M.; Sandreczki, T. C. *Polym. Mater. Sci. Eng.* **1988**, *59*, 612.
- (18) Wedgewood, A. R.; Seferis, J. C. *Pure Appl. Chem.* **1983**, *55* (5), 873.
- (19) Mijovic, J.; Andjelic, S. *Polymer* **1995**, *36* (19), 3783.
- (20) Morgan, R. J. Private communication.
- (21) England-Kretzer, L.; Fritzsche, M.; Luck, W. A. P. *J. Mol. Struct.* **1988**, *175*, 277.
- (22) Kricheldorf, H. R., Ed. *Handbook of Polymer Synthesis*; Dekker: New York, 1992.
- (23) Odian, G. *Principles of Polymerization*, 3rd ed.; Wiley: New York, 1991.

MA950550V